

BI-TP 2004/05
CERN-PH-TH/2004-025
DAMTP-2004-10
HIP-2004-05/TH
hep-lat/0402021

Duality and scaling in 3-dimensional scalar electrodynamics

K. Kajantie^a, M. Laine^b, T. Neuhaus^b, A. Rajantie^c, K. Rummukainen^{d,e,f}

^a*Theoretical Physics Division, Department of Physical Sciences,
P.O.Box 64, FIN-00014 University of Helsinki, Finland*

^b*Faculty of Physics, University of Bielefeld, D-33501 Bielefeld, Germany*

^c*DAMTP, University of Cambridge, Wilberforce Road, Cambridge CB3 0WA, UK*

^d*Department of Physics, Theory Division, CERN, CH-1211 Geneva 23, Switzerland*

^e*Department of Physics, University of Oulu, P.O.Box 3000, FIN-90014 Oulu, Finland*

^f*Helsinki Institute of Physics, P.O.Box 64, FIN-00014 University of Helsinki, Finland*

Abstract

Three-dimensional scalar electrodynamics, with a local $U(1)$ gauge symmetry, is believed to be dual to a scalar theory with a global $U(1)$ symmetry, near the phase transition point. The conjectured duality leads to definite predictions for the scaling exponents of the gauge theory transition in the type II region, and allows thus to be scrutinized empirically. We review these predictions, and carry out numerical lattice Monte Carlo measurements to test them: a number of exponents, characterising the two phases as well as the transition point, are found to agree with expectations, supporting the conjecture. We explain why some others, like the exponent characterising the photon correlation length, appear to disagree with expectations, unless very large system sizes and the extreme vicinity of the transition point are considered. Finally, we remark that in the type I region the duality implies an interesting quantitative relationship between a magnetic flux tube and a 2-dimensional non-topological soliton.

July 2004

1. Introduction

Dualities constitute one of the very few analytic tools available for studying non-perturbative properties of systems with many degrees of freedom. They have found applications in widely different physical settings, ranging from spin models to quantum field and string theories. A duality transformation typically maps topological defects to fundamental fields, and vice versa, and can therefore translate a non-perturbative problem to a solvable perturbative one, either in the same or in a different theory.

In some spin models, the duality transformation can be carried out explicitly, mapping the partition function of one theory to that of another (see, e.g., Refs. [1]–[4]). The duality is therefore a mathematical identity, and one can see exactly how the parameters and observables of the two theories relate to each other. Interacting continuum field theories, on the other hand, are generally fairly difficult to treat exactly. One reason is that they contain fluctuations on many different length scales, which do not decouple from each other, and this leads, among other things, to ultraviolet divergences. The duality may then be approximate rather than exact, and precisely valid only in a certain limit in the parameter space.

One way to limit the effect of ultraviolet divergences is to lower the dimensionality, and for instance the sine-Gordon and Thirring models in 1+1 dimensions have famously been shown to be dual to each other [5, 6]. In higher dimensions, a way to control ultraviolet divergences is to consider supersymmetric theories, where they are weak or even absent. For instance, the $\mathcal{N} = 2$ $SU(N_c)$ super-Yang-Mills theory exhibits [7] a Montonen-Olive duality [8, 9] between electric charges and magnetic monopoles. Recently there has also been a great deal of interest in dualities between the large- N_c limit of four-dimensional $\mathcal{N} = 4$ super-Yang-Mills theory and string theory in five-dimensional anti-de Sitter background [10].

Clearly, it would be interesting to extend a quantitative understanding of dualities towards dimensions closer to the physical 3+1, or to less supersymmetric theories, in order to approach, for instance, a consolidation of the 't Hooft-Mandelstam dual superconductor picture of confinement in QCD (for a recent review, see Ref. [11]). So far, however, rather few examples are available in these directions. In this paper, we study one of them, a duality between two *non-supersymmetric continuum field theories*, namely scalar electrodynamics (SQED) and complex scalar field theory (SFT), in three Euclidean dimensions [3], [12]–[20]. The duality maps the Coulomb and Higgs phases of SQED to the broken and symmetric phases of SFT, respectively. The microscopic details of the theories are not dual to each other, but as one approaches the transition point, the duality should become a better and better approximation at long distances. In principle, the duality becomes exact at the transition point (in the so-called type II region), and also describes correctly the approach to the transition point.

The nature of the duality becomes more transparent if one considers the theories in 2+1 dimensional Minkowski space. Then the duality maps the fundamental fields of one theory to vortices of the other: the vortex lines can be understood as world lines of particles in the

dual theory. One can easily make some elementary observations that hint towards the duality. First, both the Coulomb phase of SQED and the broken symmetry phase of SFT have one massless degree of freedom, namely the photon and the Goldstone mode, respectively [18], while in the other phase these degrees of freedom go over into two degenerate massive modes, in both cases. Furthermore, both the interaction between vortices in SFT and the Coulomb interaction between electric charges in SQED have the same logarithmically confining form. In contrast, the Abrikosov-Nielsen-Olesen vortices in the type II region of SQED and the fundamental particles of SFT with a positive quartic coupling, have an exponentially decreasing repulsive Yukawa interaction.

A full duality would, of course, be a stronger statement than simply a counting of the degrees of freedom, and mean that the two theories have identical dynamics as quantum systems. If all the operators allowed by the symmetries were kept in the two theories and one knew exactly the mapping between their parameters, the duality would predict that for any observable there is a corresponding observable in the dual theory with the same value. For instance, the mass spectra of the two theories should be identical.

In practice, however, one of the theories in question is truncated by dropping an infinite series of high-dimensional operators, and the exact mapping between the parameters related to the operators kept is not known, because there is no supersymmetry to cancel radiative corrections. Therefore, the best way to see the duality is to calculate universal quantities such as critical exponents, which describe the scaling properties of the system as the transition point is approached. Many critical exponents of SFT are known to a high accuracy [21], because the theory is in the same universality class as the three-dimensional XY model. The duality predicts that each of these exponents has a dual counterpart in SQED, which should have exactly the same value.¹

In this paper, we invoke previously developed numerical techniques to study topological defects [22, 23] and certain two-point functions [24, 25] in SQED, to measure a number of critical exponents with lattice Monte Carlo simulations in the type II region, and compare them with predictions following from the duality conjecture. The purpose is to demonstrate that these techniques yield results precise enough to serve as very non-trivial checks of this conjecture. The paper is organised as follows. In Sec. 2, we formulate the duality transformation and show how it relates the critical exponents of the two theories. We describe our numerical simulations and present their results in Sec. 3. In Sec. 4, we elaborate briefly on some interesting qualitative manifestations of the duality conjecture in the case of a macroscopic external magnetic field, both in the type I and in the type II regions of SQED, although we have not carried out any new simulations for this situation. Finally, we discuss our findings and present our conclusions in Sec. 5.

¹To be precise, the SQED observables we consider are sensitive only to the SFT exponent ν_{XY} as well as a certain anomalous dimension η , while for instance the exponents β_{XY}, γ_{XY} related to the response of SFT to an external magnetic field, do not play a role in the following [3].

2. Duality

2.1. Basic setup

The gauge theory under investigation, three-dimensional (3d) SQED, is formally defined by

$$\mathcal{L}_{\text{SQED}} = \frac{1}{4} F_{kl}^2 + (D_k \phi)^* (D_k \phi) + m^2 \phi^* \phi + \lambda (\phi^* \phi)^2, \quad (2.1)$$

$$\mathcal{Z}_{\text{SQED}} = \int \mathcal{D}A_k \mathcal{D}\phi \mathcal{D}\phi^* \exp\left(-\int_x \mathcal{L}_{\text{SQED}}\right), \quad (2.2)$$

where $F_{kl} = \partial_k A_l - \partial_l A_k$, $D_k = \partial_k + ieA_k$, $k, l = 1, 2, 3$, repeated indices are assumed to be summed over, and $\int_x \equiv \int d^3x$. This theory is super-renormalisable, with the only divergences appearing in the parameter m^2 . Unless otherwise stated, we assume m^2 to denote the bare parameter, and the theory to be regulated, for the moment, with dimensional regularisation. Note that all the arguments that follow are non-perturbative in nature, and there is thus no need for gauge fixing in Eq. (2.2).

While the duality relation can be expressed explicitly in a certain deformation of SQED, namely when the theory is discretised and the so-called London limit ($\lambda a \rightarrow \infty$, where a is the lattice spacing) is subsequently taken [3], [12]–[17], its status is less clear in the full continuum theory of Eqs. (2.1), (2.2), where λ is finite and $a \rightarrow 0$. In fact, the phase diagram of SQED is even qualitatively different from that of the London limit, where the transition is of the second order. In SQED the transition is of the first order if the ratio λ/e^2 is small [26] (the type I region), and is believed to be of the second order for a large λ/e^2 above the Bogomolny point (the type II region). This belief is based, apart from the apparent vicinity of the London limit, on 3d renormalisation group studies [27]–[30], previous lattice simulations [15], [31]–[35], as well as other arguments [36].²

To now formulate the duality conjecture, let us choose a specific set of observables to act as probes for the properties of the system. Defining a magnetic field through

$$B_i(x) \equiv \frac{1}{2} \epsilon_{ijk} F_{jk}(x), \quad (2.3)$$

we will mostly consider objects related to the two-point function (see also Refs. [24, 25])

$$C_{kl}(x-y) \equiv \langle B_k(x) B_l(y) \rangle. \quad (2.4)$$

To compute this kind of objects, let us generalise Eq. (2.2) and define

$$\mathcal{Z}_{\text{SQED}}[H_i] \equiv \int \mathcal{D}A_k \mathcal{D}\phi \mathcal{D}\phi^* \exp\left[-\int_x \left(\mathcal{L}_{\text{SQED}} - H_i(x) B_i(x)\right)\right], \quad (2.5)$$

where $H_i(x)$ is an arbitrary source function. The object in Eq. (2.5) is in principle well defined for a complex $H_i(x)$, but in the following we restrict ourselves to a stripe in the complex plane

²As is well known, the renormalisation group in $4 - \epsilon$ dimensions, with $\epsilon \ll 1$, continues to predict a first-order transition even at large λ/e^2 [26, 37].

where $H_i(x)$ consists of a real constant part (or zero-mode), representing a physical external magnetic field strength, and a purely imaginary space-dependent part, used as a probe to define various Green's functions. (If one wishes, the zero-mode could also be considered to be purely imaginary to start with, and analytically continued to real values only in the end, at least as long as the volume is finite.) The reason for this choice is that it turns out to simplify the form of the corresponding SFT, without posing any restrictions on the physical observables that we can address. The correlator of Eq. (2.4) is now obtained by taking the second functional derivative of $\ln \mathcal{Z}_{\text{SQED}}[H_i]$, and setting $H_i = 0$ afterwards.

The basic observation behind the duality is that SQED allows to define an exactly conserved “charge”, the magnetic flux through some surface. This conservation law can be expressed in a local form by noting that, identically,

$$\partial_i B_i(x) = 0 . \quad (2.6)$$

Thus, there should exist some global symmetry for which B_i is the Noether current [18]. This global symmetry should be broken in the “normal” Coulomb phase where the U(1) gauge symmetry is restored, the massless photon representing the Goldstone boson [18]. In the “superconducting” Higgs phase where the U(1) gauge symmetry is broken, on the other hand, the global symmetry should be restored, and the particle number of SFT, representing the number of Abrikosov-Nielsen-Olesen vortices in SQED, locally conserved.

If we were to stick to the Coulomb phase only, which has a single exactly massless degree of freedom, then the fact that an effective description exists can be made rather rigorous, following the general arguments for effective theories [38]. Once we approach the phase transition point, however, other (non-Goldstone) degrees of freedom also become massless, and the situation is less clear.

The assertion of the duality conjecture is that $\mathcal{Z}_{\text{SQED}}[H_i]$ equals the partition function of a scalar field theory (SFT), with explicit global U(1) symmetry and a mass parameter \tilde{m}^2 which is (almost) the reverse of m^2 ,

$$\tilde{m}^2 = c_0 - c_1 m^2 + \dots . \quad (2.7)$$

Here c_1 is dimensionless and positive, and c_0 is constrained by the requirement that (with a given regularisation), $\tilde{m}_c^2 = c_0 - c_1 m_c^2 + \dots$, where \tilde{m}_c^2, m_c^2 are the values of the mass parameters at the respective transition points. The quartic coupling $\tilde{\lambda}$ of SFT is also constrained:

$$\tilde{\lambda} = d_0 + d_1 \lambda + \dots , \quad (2.8)$$

where d_1 is dimensionless and positive, and d_0 is constrained by the requirement that $\tilde{\lambda}_c = d_0 + d_1 \lambda_c + \dots$, where λ_c is the “tricritical” value separating the type I and type II regions in SQED [16], while $\tilde{\lambda}_c = 0$ is the value at which scalar particles turn from attractive to

repulsive in SFT.³ The conjecture then reads that

$$\mathcal{Z}_{\text{SQED}}[H_i] = \mathcal{Z}_{\text{SFT}}[H_i], \quad (2.9)$$

where the form in which H_i appears in the partition function \mathcal{Z}_{SFT} remains to be determined.

In order to make progress, let us note that the symmetry underlying the duality can be considered to be a local one, if we assign a transformation law also to the source field H_i (cf., e.g., the analogous procedure in the case of chiral symmetry in QCD; Ref. [39] and references therein). Indeed, we can allow, in general, the source term H_i to change by a local total derivative, since this leaves $\mathcal{Z}_{\text{SQED}}$ invariant, due to Eq. (2.6), provided that the boundary integral emerging vanishes. Let us inspect this issue in some more detail.

To understand the significance of the boundary term, let us place the system in a finite box of volume V , and choose boundary conditions such that all physical fields, like $B_i(x)$, are periodic, in order to preserve translational invariance. In accordance with our choice for the analytic structure of $H_i(x)$, the transformation property of H_i has now to be purely imaginary,

$$H_i(x) \rightarrow H'_i(x) = H_i(x) - i\partial_i\alpha(x), \quad (2.10)$$

where $\alpha(x)$ is an arbitrary real function, defined, up to a so far unfixed proportionality constant, to be the generator of the local U(1) symmetry transformation. The partition function defined in Eq. (2.5) has in fact a larger symmetry than U(1), corresponding to a complex function $\alpha(x)$, but as we shall see, it is only transformations of the type in Eq. (2.10) which match the properties of the U(1) symmetry on the side of SFT. Now, since $\alpha(x)$ is not directly a physical field, we can in general consider the possibility that its boundary conditions are not strictly periodic, but are non-periodic in some direction, by an amount which we call Δ for the moment. This leads, in what one might call “large gauge transformations”, to

$$\mathcal{Z}_{\text{SQED}}[H'_i] = \mathcal{Z}_{\text{SQED}}[H_i] \exp\left[i\Delta \int d^2\mathbf{s} \cdot \mathbf{B}\right], \quad (2.11)$$

where the integral is over that boundary of the box at which $\alpha(x)$ is discontinuous by Δ . We observe that if we choose $\Delta = me$, where m is an integer, and the usual flux quantisation condition $e \int d^2\mathbf{s} \cdot \mathbf{B} = 2\pi n$, with n an integer, then the system is indeed fully invariant within each “topological” sector, characterised by n . (The whole partition function contains a sum over all the sectors). In the following we set m to its lowest non-trivial value, $m = 1$, so that the discontinuity is $\Delta = e$.

On the SFT side, then, we assume the symmetry transformation generated by $\alpha(x)$ to operate explicitly on the dual field variable, $\tilde{\phi}$:

$$\tilde{\phi} \rightarrow \tilde{\phi}' = e^{i\tilde{e}\alpha} \tilde{\phi} \quad \tilde{\phi}^* \rightarrow \tilde{\phi}'^* = e^{-i\tilde{e}\alpha} \tilde{\phi}^*, \quad (2.12)$$

³If SFT is used for describing weakly interacting atomic Bose-Einstein condensates, then the scalar self-coupling is usually written as $\tilde{\lambda} = 2\pi\hbar^2 a/m$, where a is the s-wave scattering length and m the atom mass; the transition from attractive to repulsive corresponds to the s-wave scattering length changing sign.

where we have introduced a proportionality constant \tilde{e} . We now see, first of all, that $\tilde{e}\alpha$ is defined only modulo 2π . Therefore, boundary conditions can also only be imposed modulo 2π for $\tilde{e}\alpha$, and we obtain a relation to the constant Δ introduced above,

$$\tilde{e} = \frac{2\pi}{\Delta} = \frac{2\pi}{e} . \quad (2.13)$$

Furthermore, since $\mathcal{Z}_{\text{SFT}}[H_i]$ must be invariant under the local transformation of Eqs. (2.10), (2.12) like $\mathcal{Z}_{\text{SQED}}[H_i]$ is, we can finally fix its structure:

$$\mathcal{L}_{\text{SFT}}(H_i) = \frac{1}{4} \tilde{Z} \tilde{F}_{kl}^2 + [(\partial_k - \tilde{e}H_k)\tilde{\phi}^*][(\partial_k + \tilde{e}H_k)\tilde{\phi}] + \tilde{m}^2 \tilde{\phi}^* \tilde{\phi} + \tilde{\lambda}(\tilde{\phi}^* \tilde{\phi})^2 + \dots , \quad (2.14)$$

$$\mathcal{Z}_{\text{SFT}}[H_i] = \int \mathcal{D}\tilde{\phi} \mathcal{D}\tilde{\phi}^* \exp\left[-\int_x \mathcal{L}_{\text{SFT}}(H_i)\right] , \quad (2.15)$$

where $\tilde{F}_{kl} \equiv \partial_k H_l - \partial_l H_k$.

Inspecting Eq. (2.14), we immediately obtain a physical interpretation for the duality. Choosing H_k a real constant and coordinates so that $H_k \neq 0$ only in one direction, say x_3 , which we may rename to be “imaginary time”, we note that Eqs. (2.14), (2.15) represent just the Euclidean path integral expression (cf., e.g., Ref. [40]) for a complex SFT with the chemical potential $\mu = \tilde{e}H_3$ related to the conserved current

$$\tilde{j}_k \equiv 2 \text{Im}[\tilde{\phi}^* \partial_k \tilde{\phi}] = \tilde{\phi}_1 \partial_k \tilde{\phi}_2 - \tilde{\phi}_2 \partial_k \tilde{\phi}_1 , \quad (2.16)$$

where we have written $\tilde{\phi}$ in terms of real components as $\tilde{\phi} = (\tilde{\phi}_1 + i\tilde{\phi}_2)/\sqrt{2}$. The corresponding total particle number $\int d^2\mathbf{s} \tilde{j}_3$ thus represents in SFT the same object as to which $\mu = \tilde{e}H_3$ couples in SQED, namely the integer-valued conserved flux $(e/2\pi) \int d^2\mathbf{s} \cdot \mathbf{B}$, where $d^2\mathbf{s}$ is the spatial volume element.

As we have written SFT in Eq. (2.14), it only contains a few terms. In principle, however, Eq. (2.14) should include an infinite series of (gauge invariant) higher order operators, starting with $\sim (\tilde{\phi}^* \tilde{\phi})^3$. In the type II region ($\tilde{\lambda} > 0$), they are just at most marginal, and do not modify any of the critical exponents at the transition point. In other words, their contributions are suppressed by some power of M/Λ , where M denotes the dynamical mass scales inside the truncated action of Eq. (2.14), while $\Lambda \sim e^2$ is a “confinement” scale related to excitations within 3d SQED that remain non-critical at the transition point. In the type I region ($\tilde{\lambda} < 0$), on the other hand, the higher order operators are important. In fact, $\tilde{\lambda} < 0$ together with a positive $(\tilde{\phi}^* \tilde{\phi})^3$ -term provides just the usual prototype for a first order phase transition, as is the case in the type I region. In most of the discussion that follows, we consider the type II region, and can thus ignore the higher order operators. These arguments also implicitly assume that the external magnetic field $\tilde{e}H_k$ is “small”, i.e. at most of the same order of magnitude as the dynamical mass scale M . Note that for a constant $\tilde{e}H_k$, terms like \tilde{F}_{kl}^2 vanish.

At the end of the day, the external source field H_i is often set to zero, and in that case, the Lagrangian \mathcal{L}_{SFT} of Eq. (2.14) simplifies to the standard one,

$$\mathcal{L}_{\text{SFT}} = \partial_k \tilde{\phi}^* \partial_k \tilde{\phi} + \tilde{m}^2 \tilde{\phi}^* \tilde{\phi} + \tilde{\lambda}(\tilde{\phi}^* \tilde{\phi})^2 + \dots . \quad (2.17)$$

The general form in Eq. (2.14) is still important, however, because typical predictions of the duality conjecture follow by taking functional derivatives of the equality in Eq. (2.9), and setting $H_i \rightarrow 0$ afterwards. In particular, the second functional derivative produces for our main probe, Eq. (2.4),

$$C_{kl}(x-y) = \left\{ \frac{\delta^2 \ln \mathcal{Z}_{\text{SQED}}[H_i]}{\delta H_k(x) \delta H_l(y)} \right\}_{H_i=0} \\ = \tilde{Z} \left(\square \delta_{kl} - \partial_k \partial_l \right) \delta(x-y) + 2\tilde{e}^2 \delta_{kl} \delta(x-y) \langle \tilde{\phi}^* \tilde{\phi}(x) \rangle - \tilde{e}^2 \langle \tilde{j}_k(x) \tilde{j}_l(y) \rangle + \dots, \quad (2.18)$$

where the expectation values on the right-hand side are evaluated with the Lagrangian of Eq. (2.17). Both sides of the relation in Eq. (2.18) are transverse. The constant \tilde{Z} is seen to contribute to “contact” terms only, $\sim \delta(x-y)$, but it is significant if the corresponding susceptibility (integral over all space of the two-point correlation function) is considered, which thus is not determined by the dual theory alone. Non-contact terms, on the other hand, are fully predicted in terms of the parameters of Eq. (2.17).

To conclude, we should reiterate that in certain limits, for instance when SQED is replaced with a “frozen superconductor”, or integer valued gauge theory, relations of the type in Eq. (2.18) can be made exact, for any values of the parameters (the only one being the inverse temperature β in that case) [3, 25]. In our case, on the other hand, the relations between the parameters are largely open, and the parameters even get renormalised differently in the two theories. It is only the infrared properties of the theory, that is correlations of the type in Eq. (2.18) at non-zero distances and close to the transition point, which can be related to each other, by suitably tuning the coefficients c_i in Eq. (2.7) and d_i in Eq. (2.8).

2.2. General structure of the photon two-point correlator

Defining now the Fourier transform

$$B_k(p) \equiv \int_x e^{ip \cdot x} B_k(x), \quad (2.19)$$

the object we will mostly consider is the Fourier transform of Eq. (2.4),

$$C_{kl}(p) \equiv \frac{1}{V} \langle B_k(-p) B_l(p) \rangle = \int_x e^{ip \cdot (y-x)} \langle B_k(x) B_l(y) \rangle \equiv \left(\delta_{kl} - \frac{p_k p_l}{p^2} \right) G(p), \quad (2.20)$$

where V is the volume. We choose to measure the correlator in the x_3 -direction and use a momentum transverse to that direction, $p \equiv \mathbf{p}$ (for instance, $\mathbf{p} = 2\pi n \hat{1}/L$, where $\hat{1}$ is the unit vector in the x_1 -direction, L is the linear extent of the system, and n is an integer), so that

$$C_{33}(\mathbf{p}) = G(\mathbf{p}). \quad (2.21)$$

The general structure of $G(\mathbf{p})$ is

$$G(\mathbf{p}) = \frac{\mathbf{p}^2}{\mathbf{p}^2 + \Sigma(\mathbf{p})}, \quad (2.22)$$

where, on the tree-level in SQED, the self-energy is just a constant, $\Sigma(\mathbf{p}) = m_V^2$, with m_V the inverse of the vector (or photon) correlation length. More generally, we expect that close to the critical point,

$$\Sigma(\mathbf{p}) \equiv m_\Sigma^2 + A |\mathbf{p}|^{2-\eta} + \mathcal{O}(|\mathbf{p}|^\delta), \quad (2.23)$$

where A is some (dimensionful) constant, η is the anomalous dimension, and $\delta > 2 - \eta$.

Taking a Fourier transform of Eq. (2.18), $\int_x e^{ip \cdot (y-x)}(\dots)$, we obtain now a prediction based on duality for the observable of our interest, $G(\mathbf{p})$:

$$G(\mathbf{p}) = -\tilde{Z}\mathbf{p}^2 + 2\tilde{e}^2 \langle \tilde{\phi}^* \tilde{\phi} \rangle - \tilde{e}^2 \frac{1}{V} \langle \tilde{j}_3(-\mathbf{p}) \tilde{j}_3(\mathbf{p}) \rangle + \dots. \quad (2.24)$$

The non-trivial object here, $\langle \tilde{j}_3(-\mathbf{p}) \tilde{j}_3(\mathbf{p}) \rangle$, has properties determined by SFT alone, and leads thus to a definite structure of $G(\mathbf{p})$, including corrections to scaling, etc. Formulating Eq. (2.24) in such an explicit form is, as far as we know, a new result in the present context.

In principle, Eq. (2.24) could now be used to obtain a direct prediction for the object $G(\mathbf{p})$, by inserting the numerically measured properties of SFT on the right-hand side. In practice, this is not quite straightforward, because the relations of the parameters are not fixed by the conjecture. What can be done, however, is to use Eq. (2.24) to obtain predictions for various critical exponents, since such predictions are parameter-free. SFT is known to be in the same universality class as the three-dimensional XY model, many critical exponents of which are known numerically very well [21]. Therefore, we will use them as a benchmark.

2.3. Critical exponents

While SQED in the type II region allows to define a large number of critical exponents, we will in this paper restrict only to a few of them, related in one way or the other to the “magnetic” properties of the theory, such as in Eq. (2.4). The reason is that the corresponding observables can be measured with controllable statistical and systematic errors, thanks to various numerical techniques introduced in Refs. [22]–[25], and that analytic predictions for these observables, following from the duality conjecture (through Eq. (2.24)), are unambiguous. We start by considering the symmetric phase.

Symmetric phase: magnetic permeability. Magnetic permeability can be defined by considering a constant source $H_3 \equiv H$, and the response of the magnetic field strength $B \equiv V^{-1} \int_x B_3(x)$ to H ,

$$\chi \equiv \frac{\partial B}{\partial H} = \frac{1}{V} \frac{\partial^2}{\partial H^2} \ln \mathcal{Z}_{\text{SQED}} = \lim_{\mathbf{p} \rightarrow 0} G(\mathbf{p}). \quad (2.25)$$

In the free Abelian theory we would have $H = B$ and $\chi = 1$, as can be seen by setting $\Sigma \rightarrow 0$ in Eq. (2.22), or directly by starting from the free energy $F(B) = \frac{1}{2} B^2 V$. When interactions

are taken into account, 1-loop perturbation theory at large m^2 gives [33]

$$\chi \approx 1 - \frac{e^2}{24\pi\sqrt{m^2(\bar{\mu})}} + \dots, \quad (2.26)$$

where $m^2(\bar{\mu})$ is the renormalised mass parameter in dimensional regularisation (in the $\overline{\text{MS}}$ scheme, for concreteness). Thus, χ decreases as we approach the transition point $m^2(\bar{\mu}) \sim 0$.

To understand the critical behaviour of χ , note that in the broken phase of SFT, the correlator $\langle \tilde{j}_k(-p)\tilde{j}_l(p) \rangle$ is dominated by the massless Goldstone mode, so that $\langle \tilde{j}_k(-p)\tilde{j}_l(p) \rangle \propto \langle \tilde{\phi}^*\tilde{\phi} \rangle p_k p_l / p^2$, and consequently

$$\lim_{\mathbf{p} \rightarrow 0} \langle \tilde{j}_3(-\mathbf{p})\tilde{j}_3(\mathbf{p}) \rangle = 0. \quad (2.27)$$

Thus the duality in Eq. (2.24) predicts that

$$\chi = 2\tilde{e}^2 \langle \tilde{\phi}^*\tilde{\phi} \rangle. \quad (2.28)$$

Essentially the same argument was presented recently by Son [20]: he considered an effective theory for the Goldstone mode alone, $\phi(x) \equiv (1/\sqrt{2})f \exp(i\alpha(x))$, and thus obtained $\chi = \tilde{e}^2 f^2$, where f^2 is the helicity modulus, or stiffness, or decay parameter, related to the Goldstone mode, and equals $2\langle \tilde{\phi}^*\tilde{\phi} \rangle$ in our notation. Note that we have implicitly assumed the use of continuum (dimensional) regularisation in writing down the duality relation, and Eq. (2.28) should also be understood to be correspondingly regularised.

There are various ways to derive the critical scaling exponent of $\langle \tilde{\phi}^*\tilde{\phi} \rangle$. For instance, given that the action contains $S_{\text{SFT}} \sim \int d^3x \partial_k \tilde{\phi}^* \partial_k \tilde{\phi}$, we may dimensionally expect [41] that $\langle \tilde{\phi}^*\tilde{\phi} \rangle \sim 1/|x| \sim 1/\xi_{\text{SFT}} \sim |\tau|^{\nu_{XY}}$, where we have introduced the distance from the critical point, τ , by

$$\frac{m^2 - m_c^2}{e^4} \equiv \tau. \quad (2.29)$$

Other arguments leading to the same result can be put forward (Ref. [20] and references therein), and will also be met below. Thus, if $\chi(\tau) \sim |\tau|^{\nu_\chi}$ for $\tau \rightarrow 0^+$, we obtain [20]

$$\nu_\chi = \nu_{XY}, \quad (2.30)$$

where ν_{XY} is the exponent of the correlation length ξ_{SFT} in SFT.

To test this critical behaviour we can devise, following [24], a finite-size scaling procedure for measuring the exponent. Close to the critical point, for box sizes larger than the correlation length ξ of non-Goldstone modes, the system behaves as if it were almost in infinite volume, so that ($\mathbf{p}_{\text{min}} \equiv 2\pi\hat{1}/L$)

$$\Sigma(\mathbf{p}_{\text{min}}) = \chi^{-1}(\tau)\mathbf{p}_{\text{min}}^2 + \mathcal{O}(\mathbf{p}_{\text{min}}^4). \quad (2.31)$$

For box sizes smaller than ξ (but still large compared with the microscopic scales), on the other hand, the system behaves as if it were already at the critical point,

$$\Sigma(\mathbf{p}_{\text{min}}) = A\mathbf{p}_{\text{min}}^{2-\eta} + \mathcal{O}(\mathbf{p}_{\text{min}}^\delta). \quad (2.32)$$

Therefore,

$$\mathbf{p}_{\min}^\eta G^{-1}(\mathbf{p}_{\min}) \sim \mathbf{p}_{\min}^{\eta-2} \Sigma(\mathbf{p}_{\min}) \sim \begin{cases} |\tau|^{-\nu_\chi} L^{-\eta} & , \quad L \gtrsim \xi \\ A & , \quad L \lesssim \xi \end{cases} . \quad (2.33)$$

The function has to be continuous at $L \sim \xi \sim |\tau|^{-\nu_\chi}$; thus, using Eq. (2.30), $\eta = 1$. The functional form close to the critical point should be universal, and according to Eq. (2.33) for $\eta = 1$, only dependent on $|\tau|L^{1/\nu_\chi}$:

$$\mathbf{p}_{\min} G^{-1}(\mathbf{p}_{\min}) \sim f(|\tau|L^{1/\nu_\chi}) , \quad (2.34)$$

with $f(x) = A$, $x \ll 1$, and $f(x) \sim x^{-\nu_\chi}$, $x \gg 1$. Subsequently at the critical point, $|\tau| \rightarrow 0$, it has a fixed point value, A . Moreover, if we take a derivative with respect to τ at the critical point, we obtain

$$\frac{d}{d\tau} [\mathbf{p}_{\min} G^{-1}(\mathbf{p}_{\min})]_{\tau=0} \sim L^{1/\nu_\chi} . \quad (2.35)$$

Eq. (2.35) will be used below to measure ν_χ , as was done in Ref. [24] for a related model.

Transition point: anomalous dimension. In the previous paragraph, we already found a specific value for the anomalous dimension η , $\eta = 1$, assuming that the magnetic permeability scales with the same exponent as the correlation length, as argued in Eq. (2.30). Let us now show that the same value for the anomalous dimension can be obtained without any assumption for the behaviour of $\chi(\tau)$. The reasoning could then be reversed, to provide yet more evidence for the scaling of $\chi(\tau)$ according to Eq. (2.30).

The anomalous dimension related to $G(\mathbf{p})$ can be found in a particularly simple way with an argument similar to one by Son [20]. Let us consider $\mathcal{Z}_{\text{SFT}}[H_i]$ at the transition point. Factoring out the term multiplied by \tilde{Z} , the system should be ‘‘conformally invariant’’ at the critical point, or have no scales. For dimensional reasons, the quadratic part of $\ln \mathcal{Z}_{\text{SFT}}$, which is a function of $\tilde{e}H_i$ only, must thus have the structure

$$\ln \mathcal{Z}_{\text{SFT}}[H_i] \propto \int_p \left(\delta_{kl} - \frac{p_k p_l}{p^2} \right) [\tilde{e}H_k(-p)] [\tilde{e}H_l(p)] |p| , \quad (2.36)$$

where $\int_p = \int d^3p / (2\pi)^3$. Using this to compute $G(\mathbf{p})$ through the Fourier transform of the second functional derivative of $\ln \mathcal{Z}_{\text{SFT}}$, like in Eqs. (2.18), (2.20), (2.24), and comparing with Eq. (2.23) for $m_\Sigma^2 = 0$, it follows that $\eta = 1$.

The structure of Eq. (2.36) can also be found with a perturbative 1-loop computation. On the side of SQED, the computation was carried out in Ref. [42] in the Coulomb phase, with the result ⁴

$$\Sigma(\mathbf{p}) = \frac{1}{16} e^2 |\mathbf{p}| , \quad \text{for } \mathbf{p}^2 \gg m^2(\bar{\mu}) . \quad (2.37)$$

Higher loop corrections are non-vanishing, however, and even diverge at the critical point $m^2(\bar{\mu}) \sim 0$, whereby there is really no hard prediction for the critical exponent. On the

⁴Wilson-type renormalisation group studies in SQED lead to the same functional behaviour [28, 29].

other hand, one could also carry out the computation on the side of SFT, as we just did, and possibly combine with the Wilson renormalisation group there: this line of reasoning can in principle also be used to understand that $\eta = 1$ (see, e.g., Ref. [19]). For a lattice study within a certain version of the dual theory, again leading to $\eta = 1$, see Ref. [43].

Broken symmetry phase: inverse vector propagator at zero momentum. The quantity we will measure in the broken symmetry phase is the infrared limit of the inverse of the vector propagator,

$$\lim_{\mathbf{p} \rightarrow 0} \mathbf{p}^2 G^{-1}(\mathbf{p}) = \lim_{\mathbf{p} \rightarrow 0} \Sigma(\mathbf{p}) \equiv m_\Sigma^2. \quad (2.38)$$

Our aim is to determine the exponent associated with m_Σ^2 , $m_\Sigma^2 \sim |\tau|^{\gamma_\Sigma}$. To relate γ_Σ to more physical quantities, note that according to Eq. (2.23), for small \mathbf{p} and m_Σ^2 the structure of the inverse propagator should be

$$\mathbf{p}^2 G^{-1}(\mathbf{p}) \sim m_\Sigma^2 + A|\mathbf{p}|^{2-\eta}. \quad (2.39)$$

Therefore the inverse of the physical vector correlation length, or the “photon mass” m_V , which is defined by the position of the singularity in $G(\mathbf{p})$, or zero in $\mathbf{p}^2 G^{-1}(\mathbf{p})$, scales as

$$m_V = |\mathbf{p}_{\text{pole}}| \sim (m_\Sigma^2)^{\frac{1}{2-\eta}} \sim |\tau|^{\nu_V} \quad \Leftrightarrow \quad \nu_V = \frac{\gamma_\Sigma}{2-\eta}. \quad (2.40)$$

Thus, a determination of γ_Σ combined with the known η amounts to a determination of ν_V . Conversely, given a prediction for ν_V , as follows in the next paragraph, we have a prediction for γ_Σ [24], which will be tested below.

Broken symmetry phase: vector correlation length. As just mentioned, the vector correlation length is determined by the position of the singularity in $G(\mathbf{p})$. According to Eq. (2.24), it is determined in SFT by the singularity structure in the current–current correlator in the symmetric phase. Since the current represents a two-particle state ($\sim \tilde{\phi}_1 \partial \tilde{\phi}_2$, cf. Eq. (2.16)), it is natural to expect that the singularity is placed at the two-particle threshold, $m_V = 2M$, where M denotes the inverse of the scalar correlation length; this is certainly the behaviour obtained with a 1-loop computation in SFT. Therefore, we expect that

$$m_V = 2M \sim 2|\tau|^{\nu_{XY}}, \quad (2.41)$$

i.e., $\nu_V = \nu_{XY}$ [29, 19]. Returning now back to Eq. (2.40) and inserting $\eta = 1$, we also find that [24]

$$\gamma_\Sigma = \nu_{XY}. \quad (2.42)$$

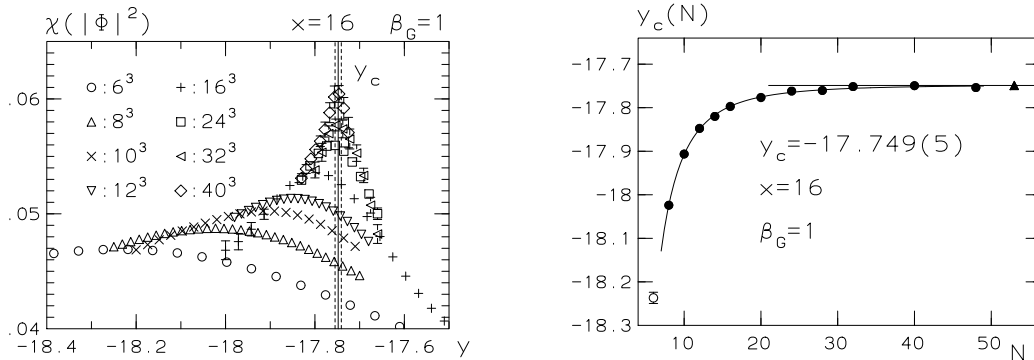


Figure 1: Left: Examples of reweighted susceptibilities $\chi(|\hat{\phi}|^2)$. Right: Determination of the infinite volume critical point y_c (triangle) from the positions of the susceptibility maxima.

Broken symmetry phase: vortex tension. Consider finally the vortex tension. Following again an elegant argument by Son [20], let us consider the effect of a constant $H_3 \equiv H$ on the gauge theory side. Because of the Meissner effect, the system does not respond ($\mathcal{Z}_{\text{SQED}}$ does not change) until $H \geq H_{c1} = eT/2\pi$, where T is the tension of an infinitely long vortex. On the SFT side, on the other hand, a constant $\tilde{e}H$ corresponds to a relativistic chemical potential μ in a (2+1)-dimensional theory, $\mu = \tilde{e}H$. Therefore, the system does not respond until $\mu \geq M$, where M is the particle mass. We thus obtain $M = \tilde{e}H_{c1} = T$, i.e., that the vortex tension should again scale with the same exponent ν_{XY} as M does: if $T \sim |\tau|^{\nu_T}$, then

$$\nu_T = \nu_{XY} . \quad (2.43)$$

3. Simulations

3.1. Discretised action

We discretise the action in Eq. (2.1) in a standard way, by replacing

$$F_{kl}(\mathbf{x}) \rightarrow \frac{1}{ea^2} \left[\alpha_k(\mathbf{x}) + \alpha_l(\mathbf{x} + a\hat{k}) - \alpha_k(\mathbf{x} + a\hat{l}) - \alpha_l(\mathbf{x}) \right] \equiv \frac{1}{ea^2} \alpha_{kl}(\mathbf{x}) , \quad (3.1)$$

$$D_k \phi \rightarrow \frac{1}{a} \left[\exp(i\alpha_k(\mathbf{x})) \phi(\mathbf{x} + a\hat{k}) - \phi(\mathbf{x}) \right] , \quad (3.2)$$

$$\int d^3\mathbf{x} \rightarrow \sum_{\mathbf{x}} a^3 , \quad (3.3)$$

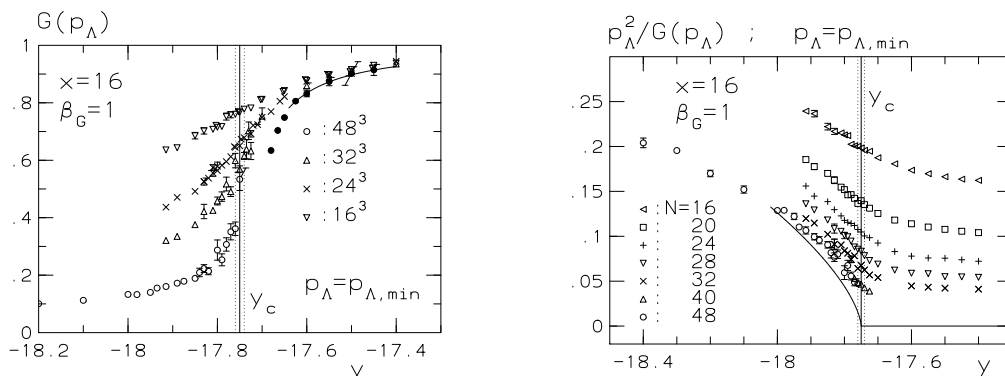


Figure 2: Left: The behaviour of $G(\mathbf{p}_{\min})$ at a few representative volumes. The filled circles and the solid curve correspond to the infinite volume limit. Right: The function $\mathbf{p}_{\min}^2 G^{-1}(\mathbf{p}_{\min})$. The solid curve corresponds to the infinite volume limit.

where a is the lattice spacing, \hat{k}, \hat{l} are unit vectors, and $\alpha_i(\mathbf{x}) = aeA_i(\mathbf{x})$.⁵ The bare mass parameter is written in a form which guarantees that the $\overline{\text{MS}}$ renormalised mass parameter $m^2(\bar{\mu})$, evaluated at the scale $\bar{\mu} = e^2$, remains finite in the continuum limit [46]:

$$m^2 \equiv m^2(e^2) - (e^2 + 2\lambda) \frac{3.175911535625}{2\pi a} - \frac{1}{16\pi^2} \left[(-4e^4 + 8\lambda e^2 - 8\lambda^2) \left(\ln \frac{6}{ae^2} + 0.08849 \right) - 1.1068e^4 + 4.6358\lambda e^2 \right]. \quad (3.4)$$

The couplings e^2, λ , on the other hand, do not require renormalisation in three dimensions (for $\mathcal{O}(a)$ -corrections, see Ref. [47]). Once we also rewrite $\phi \equiv e\hat{\phi}$, the action becomes dimensionless, parameterised only by

$$x \equiv \frac{\lambda}{e^2}, \quad y \equiv \frac{m^2(e^2)}{e^4}, \quad \beta_G \equiv \frac{1}{e^2 a}. \quad (3.5)$$

The continuum limit corresponds to $\beta_G \rightarrow \infty$. Instead of Eq. (2.29), we can now write

$$\tau = y - y_c. \quad (3.6)$$

The fields that are updated are the real variables $\alpha_k(\mathbf{x})$ and the complex ones $\hat{\phi}(\mathbf{x})$. For details concerning the update algorithm employed in this work, we refer to Refs. [22, 23]. Once the system is put on the lattice, one also has to impose boundary conditions. In the following paragraphs we employ periodic boundary conditions for all the fields. This implies that the net winding (or flux) through the lattice in any configuration, $w \equiv e \int d^2 \mathbf{s} \cdot \mathbf{B}$, vanishes, rather

⁵Note that in Eq. (3.1) we use the non-compact formulation for the U(1) gauge field. We do this to avoid topological artifacts, monopoles, which appear in the so-called compact formulation [44], unless $e^2 a \ll 1$, and would make it difficult to reach large volumes in physical units, i.e. $V \gg 1/e^6$ [45].

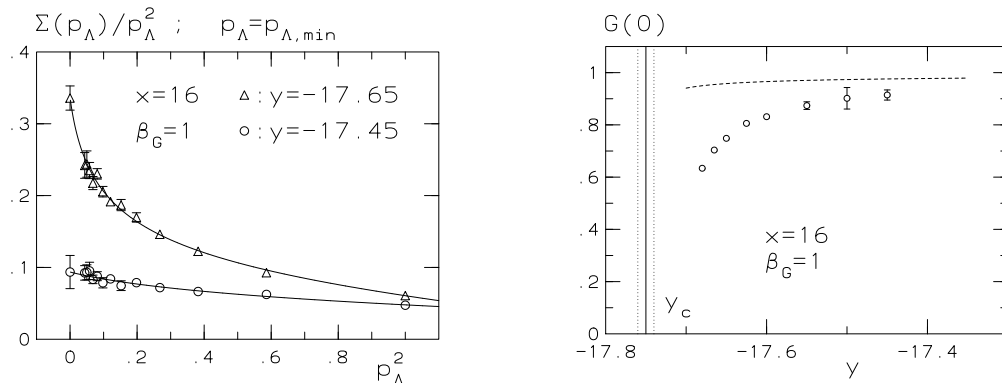


Figure 3: Left: Examples of infinite volume extrapolations for $\mathbf{p}_{\min}^{-2}\Sigma(\mathbf{p}_{\min})$ in the symmetric phase. We fit to the 1-loop perturbative expression, with the mass of the scalar particle as a free parameter. The extrapolation range increases rapidly while approaching the critical point. Right: The corresponding behavior for $G(0) = \lim_{\mathbf{p}_{\min} \rightarrow 0} [1 + \mathbf{p}_{\min}^{-2}\Sigma(\mathbf{p}_{\min})]^{-1}$. The dashed line represents the perturbative prediction in Eq. (2.26), with $m^2(\bar{\mu}) \rightarrow (y - y_c)e^4$.

than fluctuates as it in principle should in the canonical ensemble of Eq. (2.5). At the critical point this choice affects some quantities, like amplitude ratios, but it is not expected to affect the critical exponents on which we concentrate here.

The observables are discretised in a straightforward way. In particular, denoting again $\mathbf{p} = 2\pi n\hat{1}/L$, the quantity $G(\mathbf{p})$ in Eq. (2.21) is measured as

$$G(\mathbf{p}) \equiv \beta_G \sum_{\mathbf{x}} e^{i\mathbf{p}\cdot\mathbf{x}} \langle \alpha_{12}(0)\alpha_{12}(\mathbf{x}) \rangle . \quad (3.7)$$

In the figures we always plot the momentum in the form in which it appears in discrete space,

$$p_\Lambda \equiv \frac{2}{a} \sin \frac{a|\mathbf{p}|}{2} , \quad p_{\Lambda, \min} \equiv \frac{2}{a} \sin \frac{a|\mathbf{p}_{\min}|}{2} = \frac{2}{a} \sin \frac{\pi}{N} , \quad (3.8)$$

where \mathbf{p} was assumed to point along the x_1 -axis, and the lattice size was denoted by $L = Na$. We often use furthermore lattice units, $a = 1$.

3.2. Simulation parameters

All the simulations in this paper have been carried out with a single lattice spacing, $\beta_G = 1$. The reason is that since we are interested in universal critical behaviour and are using the non-compact formulation, there is no need for a continuum extrapolation, as long as there is no phase transition in between the β_G used and $\beta_G = \infty$; this indeed is the case. The scalar coupling is chosen to lie comfortably in the type II region (i.e., beyond the Bogomolny point, $x = 1/2$), $x = 16$. We have also performed some simulations at $x = 2$, which still lies in the type II region [34], confirming the qualitative pattern observed at $x = 16$ but with

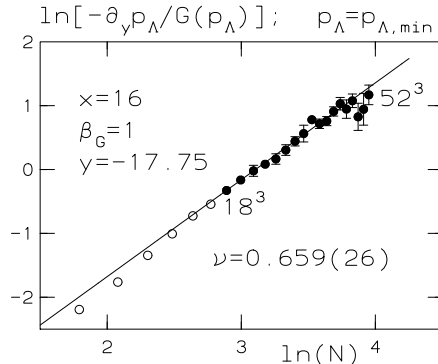


Figure 4: The derivative $-\partial_y[\mathbf{p}_{\min}G^{-1}(\mathbf{p}_{\min})]$ at the critical point, as a function of the volume, and a determination of the exponent of magnetic permeability via Eq. (2.35).

significantly less resolution. Volumes have been chosen in the range $6^3 \dots 52^3$, and for each parameter value we collect from $\sim 10^5$ to $\sim 2 \times 10^6$ sweeps. Different parameter values are joined together with Ferrenberg-Swendsen multihistogram reweighting [48].

3.3. Location of the critical point

The first task is to locate the critical point, y_c . While there are many possibilities for doing this, all are in principle equivalent in the limit $V \rightarrow \infty$, and we choose here to use the location of the maximum of the “specific heat”, or the susceptibility related to $|\hat{\phi}|^2$,

$$\chi(|\hat{\phi}|^2) \equiv N^3 \left[\langle (|\overline{\phi}|^2)^2 \rangle - \langle |\overline{\phi}|^2 \rangle^2 \right], \quad (3.9)$$

where $|\overline{\phi}|^2 \equiv V^{-1} \int_x \hat{\phi}^* \hat{\phi}$. Our data at a few representative volumes are shown in Fig. 1(left), and an infinite volume extrapolation based on the positions of the susceptibility maxima in Fig. 1(right). The extrapolation has been carried out with the finite-size scaling ansatz

$$y_c(N = \infty) = y_c(N) + c_1 \frac{1}{N^{1/\nu}} + c_2 \frac{1}{N^{1/\nu+\omega}} + \dots, \quad (3.10)$$

where the exponents have been fixed to their SFT values, $\nu \equiv \nu_{XY} = 0.67155(27)$, $\omega \equiv \omega_{XY} = 0.79(2)$ [21]. We find

$$y_c = -17.749(5). \quad (3.11)$$

This value will be frequently referred to below, in the form $y_c \approx -17.75$.

The critical point is of course clearly visible also in the observable we are actually interested in, $G(\mathbf{p})$. In Fig. 2 we show the structure of $G(\mathbf{p}_{\min})$ (left) and $\mathbf{p}_{\min}^2 G^{-1}(\mathbf{p}_{\min})$ (right), with $\mathbf{p}_{\min} = 2\pi\hat{1}/L$. Both become order parameters in the infinite volume limit $\mathbf{p}_{\min} \rightarrow 0$, vanishing on one side of y_c .

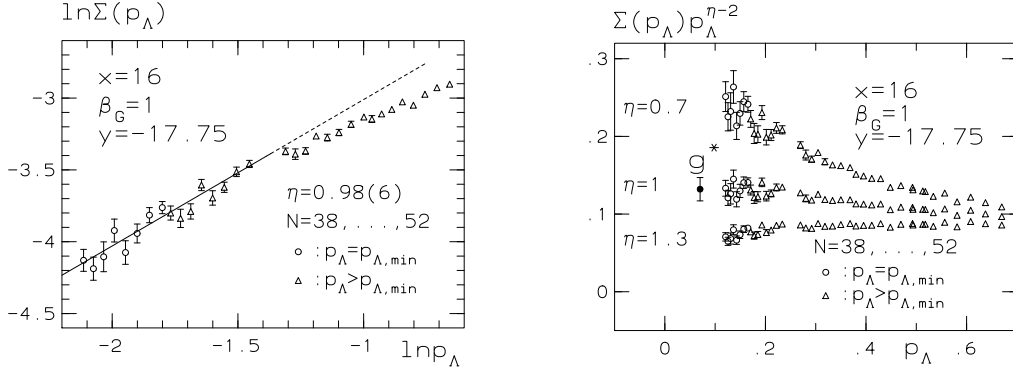


Figure 5: Left: The photon self-energy $\Sigma(\mathbf{p})$ at the critical point. Circles denote momenta $|\mathbf{p}_{\min}| = 2\pi/L$ at different volumes; triangles denote larger momenta. The solid curve is a linear fit determining the anomalous dimension η . Right: An alternative determination of η as well as of the fixed-point coefficient g^* (cf. Fig. 6), based on Eq. (2.33).

3.4. Symmetric phase: magnetic permeability

The magnetic permeability, as defined in Eq. (2.25), could in principle be determined directly from an infinite volume ($\mathbf{p}_{\min} \rightarrow 0$) extrapolation of the data in Fig. 2(left). Such an extrapolation cannot be carried out in practice, however, because the function approaches its infinite volume limit very slowly close to the critical point. This is illustrated in Fig. 3(left) at two selected y -values well inside the Coulomb phase, $y > y_c$. The corresponding extrapolated values are shown in Fig. 3(right) (without any estimate of the systematic uncertainties introduced by the extrapolation), but are reliably extracted only so far above y_c that no meaningful fit for a critical exponent can be carried out.

Fortunately, we can determine the exponent directly, by carrying out a finite-size scaling study exactly at $y = y_c$, employing Eq. (2.35). In order to measure the derivative, we construct explicitly the corresponding operator,

$$\begin{aligned}
 -\frac{d}{dy}G^{-1} &= \frac{1}{G^2} \frac{d}{dy}G = -\frac{1}{G^2\beta_G^2} \left[\left\langle \sum_{\mathbf{x}} e^{i\mathbf{p}\cdot\mathbf{x}} \alpha_{12}(0) \alpha_{12}(\mathbf{x}) \sum_{\mathbf{y}} \hat{\phi}^*(\mathbf{y}) \hat{\phi}(\mathbf{y}) \right\rangle \right. \\
 &\quad \left. - \left\langle \sum_{\mathbf{x}} e^{i\mathbf{p}\cdot\mathbf{x}} \alpha_{12}(0) \alpha_{12}(\mathbf{x}) \right\rangle \left\langle \sum_{\mathbf{y}} \hat{\phi}^*(\mathbf{y}) \hat{\phi}(\mathbf{y}) \right\rangle \right]. \quad (3.12)
 \end{aligned}$$

The data are shown in Fig. 4(left), and a fit to the filled circles produces a value

$$\nu_\chi = 0.659(26). \quad (3.13)$$

This is well consistent with the SFT value $\nu_{XY} = 0.67$, as predicted by Eq. (2.30).

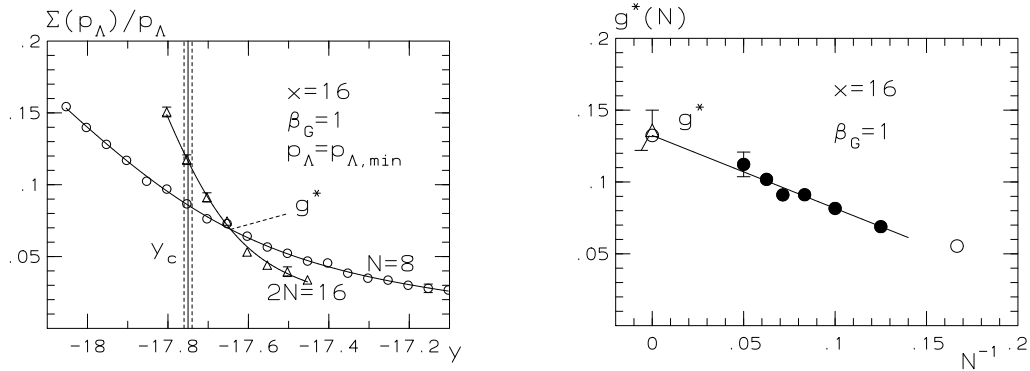


Figure 6: Left: Determination of the fixed point value of the photon self-energy from the function $\Sigma(\mathbf{p}_{\min})/|\mathbf{p}_{\min}|$, by a comparison of two volumes. Right: An extrapolation to infinite volume and a comparison with the determination of g^* in Fig. 5 (open triangle).

3.5. Transition point: anomalous dimension

Our next task is to determine the anomalous dimension. In Fig. 5(left), we do this directly through Eq. (2.32), with $\Sigma(\mathbf{p})$ extracted from the measured $G(\mathbf{p})$ (Eq. (3.7)) via Eq. (2.22). A fit to the data at \mathbf{p}_{\min} produces

$$\eta = 0.98(6), \quad (3.14)$$

in perfect agreement with the prediction following from Eq. (2.36).

An alternative determination of η can be obtained by using Eq. (2.33). In Fig. 5(right), we show $\Sigma(\mathbf{p}_{\min})\mathbf{p}_{\min}^{\eta-2}$ at $y = y_c$, observing that a fixed-point value in the infinite-volume ($\mathbf{p}_{\min} \rightarrow 0$) limit is only obtained with $\eta \approx 1$. We have also estimated the fixed-point value g^* of $\Sigma(\mathbf{p}_{\min})/\mathbf{p}_{\min}$, corresponding to A/e^2 in the notation of Eq. (2.33).⁶

The fact that the function $\Sigma(\mathbf{p}_{\min})/\mathbf{p}_{\min}$ approaches a fixed-point value, allows also for an alternative determination of g^* . Indeed, following the standard procedure, we can estimate the infinite-volume limit by comparing data for $\Sigma(\mathbf{p}_{\min})/\mathbf{p}_{\min}$ at two lattice sizes, N and $2N$, for various N . The procedure is illustrated in Fig. 6(left), and produces values for g^* (cf. Fig. 6(right)) consistent with but more precise than in Fig. 5(right): in the limit $N \rightarrow \infty$, a linear fit yields $g^* \approx 0.13(1)$. This value will find applications in Sec. 3.7.

3.6. Broken symmetry phase: inverse vector propagator at zero momentum

We next consider the parameter m_Σ^2 , defined in Eq. (2.38). The infinite-volume extrapolation of $\mathbf{p}_{\min}^2 G^{-1}(\mathbf{p}_{\min})$ is illustrated in Fig. 7(left), and a fit as a function of y is shown in

⁶The fixed-point value g^* , unlike critical exponents, is possibly sensitive to the boundary conditions used. Let us reiterate that our simulations at this point correspond to a vanishing winding (or flux), $w = 0$.

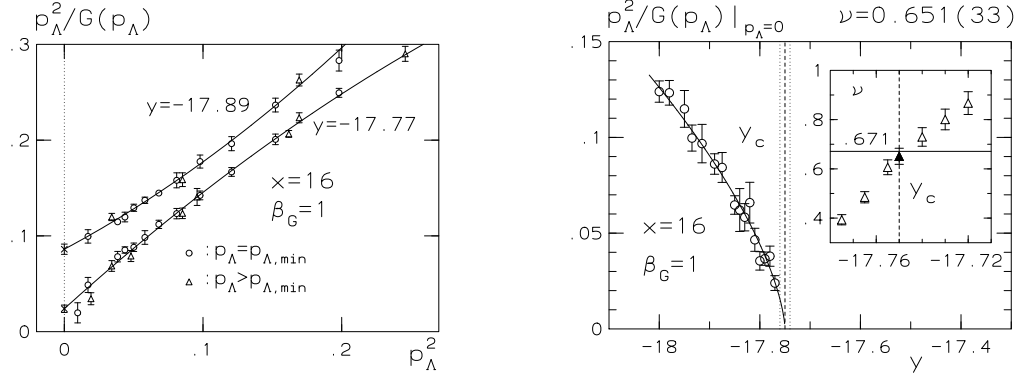


Figure 7: Left: Infinite volume extrapolations for $\mathbf{p}^2 G^{-1}(\mathbf{p})$ at two values of y in the broken symmetry phase. Circles denote momenta $|\mathbf{p}_{\min}| = 2\pi/L$ at different volumes; triangles denote larger momenta. Right: The scaling behavior for the infinite volume extrapolated $\mathbf{p}^2 G^{-1}(\mathbf{p})$. The inlay shows the dependence of the critical exponent on the value of y_c .

Fig. 7(right). We find

$$\gamma_\Sigma = 0.651(33) , \quad (3.15)$$

in perfect agreement with Eq. (2.42).

3.7. Broken symmetry phase: vector correlation length

Let us then discuss the vector correlation length. As reported earlier on [33, 35], direct measurements of the vector correlation function struggle to show critical behaviour according to the exponent ν_{XY} as predicted by Eq. (2.41), producing rather the exponent $\nu_{XY}/2$. In the light of the data presented in this paper, however, such a behaviour is well understandable. Indeed, close to the critical point the form of the vector propagator is as shown in Eqs. (2.22), (2.23), with $\eta = 1$. We have just determined that $A \approx g^* e^2 \approx 0.13e^2$. This means that in order for true critical behaviour to show up in infinite volume, we would need to require

$$m_V^2 \ll 0.13e^2 m_V , \quad \text{or} \quad m_V \ll 0.13e^2 . \quad (3.16)$$

This is the case, however, only extremely close to the transition point (cf. Fig. 2 in Ref. [35]). Moreover, even when $m_V \approx 0$, finite-volume corrections to the asymptotic form of the photon correlator are important, unless

$$\mathbf{p}_{\min}^2 \ll 0.13e^2 \mathbf{p}_{\min} , \quad (3.17)$$

which at $\beta_G = 1$ transforms to

$$N \gg \frac{2\pi}{0.13} \approx 48 . \quad (3.18)$$

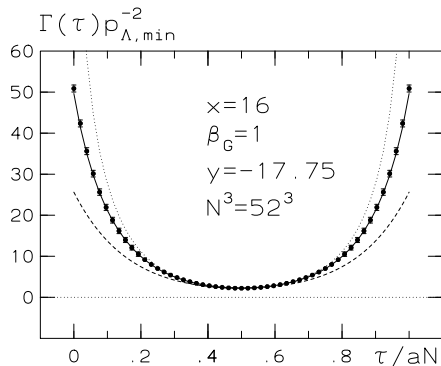


Figure 8: The photon correlation function at the critical point, with transverse momentum \mathbf{p}_{\min} , compared with a Fourier transform of $1/[p^2 + A|p|]$ (solid; cf. Eqs. (2.22), (2.23)), as well as with Fourier transforms of $1/p^2$ (dashed), $1/|p|$ (dotted), in each case with an overall constant chosen so that data points are matched at $\tau/aN = 0.5$.

It is not easy to satisfy this inequality in practice, however. Away from the transition point $m_V \approx 0$, or in volumes smaller than Eq. (3.18), on the other hand, the free term \mathbf{p}^2 will dominate the inverse vector propagator in Eq. (2.22), and solving for the pole position with the free part alone, we recover the exponent

$$\nu_V^{(\text{effective})} \approx \frac{1}{2} \gamma_\Sigma = \frac{1}{2} \nu_{XY}. \quad (3.19)$$

For completeness, the highly non-trivial form of the vector correlation function is illustrated in Fig. 8 at $y = y_c$. It is seen clearly how the free term \mathbf{p}_{\min}^2 and the linear term in $\Sigma(\mathbf{p}_{\min})$ are both needed in order to reproduce the data points, even at volumes as large as 52^3 .

If the mapping between the parameters of SQED and SFT were known, one would not need to rely on the asymptotic critical behaviour to demonstrate the duality between the two theories, but one could compare the data directly, staying away from the transition point and keeping the volume finite. Without the mapping such a comparison is not available on a quantitative level, but we may still note that the data obtained for the vector correlation length in the “frozen superconductor” model, where the duality is exact, show a behaviour very similar to what we have argued for here and observed in Refs. [33, 35], i.e. $\nu_{XY}/2 \lesssim \nu_V^{\text{effective}} < \nu_{XY}$, at least apart from the extreme vicinity of the transition point [25]. This provides further qualitative support for the duality conjecture, through similar corrections to asymptotic scaling in both theories.

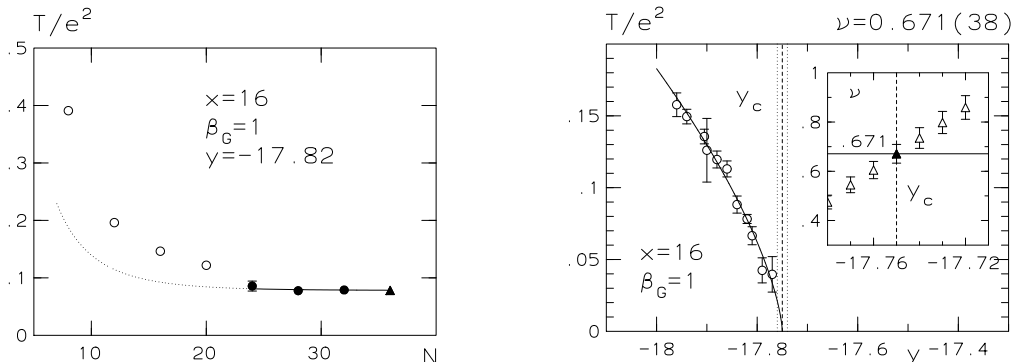


Figure 9: Left: An example of an infinite volume extrapolation (triangle) for the tension T/e^2 in the broken symmetry phase. The ansatz is as explained in Ref. [23], and is only applicable in large volumes (solid curve). Right: The scaling behavior for the infinite volume extrapolation. The inlay shows the dependence of the critical exponent on the value of y_c .

3.8. Broken symmetry phase: vortex tension

We finally consider the vortex tension, T .⁷ Unlike for the observables so far, its determination requires that we depart from strictly periodic boundary conditions for all the fields. In fact, the Monte Carlo determination of T proceeds via a computation of the free energy difference $\ln \mathcal{Z}_{\text{SQED}}(w = 0) - \ln \mathcal{Z}_{\text{SQED}}(w = 2\pi)$, where the winding number $w = e \int d^2\mathbf{s} \cdot \mathbf{B} = 2\pi$ corresponds to the presence of a single vortex through the lattice. Parametrizing $w = 2\pi z$, we can write $\ln \mathcal{Z}_{\text{SQED}}(w = 2\pi) = \ln \mathcal{Z}_{\text{SQED}}(0) + \int_0^1 dz \langle W(z) \rangle$, where $\langle W(z) \rangle$ represents a specific expectation value, which can be measured by Monte Carlo methods. For more details, we refer the reader to our earlier work [22, 23].

In the earlier work mentioned, the integral $\int_0^1 dz \langle W(z) \rangle$ was approximated by a sum over independent and consecutive Monte Carlo measurements at a discrete set z_i , $i = 1, \dots, n_z$, where the parameter n_z had typically values $n_z = 11, \dots, 21$. For the current work, we have implemented “parallel tempering” in the parameters z_i , along the lines of Ref. [49], in an attempt to sample intermediate configurations with non-integer winding numbers $0 < z < 1$ more efficiently. Using again $n_z = 21$, we find a sizable error reduction, as compared with our earlier approach. This is illustrated by the single data point with large error bars in Fig. 9(right), at $y \approx -17.9$, obtained with the unimproved algorithm. We have not investigated the precise mechanism behind this algorithmic improvement in great detail, however.

In Fig. 9(left) we show an example of the infinite volume extrapolation of the tension in

⁷We use the same notation for the vortex tension and the temperature, but there should be no danger of confusion, since the two are never discussed in the same context.

the broken phase, and in Fig. 9(right) a fit to the extrapolated values. The fit yields

$$\nu_T = 0.671(38) , \quad (3.20)$$

in perfect agreement with Eq. (2.43).

4. Macroscopic external magnetic fields

Up to this point, we have mostly considered the case that the magnetic field is set to zero, $H_i = 0$, after taking derivatives of the partition function (cf. Eq. (2.18)); the main exception was the discussion of the vortex tension, leading to Eq. (2.43) and continued in Sec. 3.8. In this section, we wish to make some further qualitative remarks on the case that the external magnetic field is not set to zero but kept finite.

To begin with, let us reiterate the duality relation for this situation, in rather explicit form. We choose again coordinates such that the constant magnetic field is pointing in the third direction, $H_3 \equiv H$, and consider the system to live in a finite box (or hypertorus), now of extent L in the third direction. Then $\mathcal{Z}_{\text{SQED}}[H]$ represents the *classical* Euclidean partition function for *3-dimensional* SQED, with the external parameters H, L . At the same time, the corresponding $\mathcal{Z}_{\text{SFT}}[H]$, Eqs. (2.14), (2.15), is just the imaginary time *quantum* partition function for a *2-dimensional* SFT, in the presence of a finite chemical potential $\mu = \tilde{e}H$ (written in a relativistic form) and a finite temperature T (fixed by the extent of the imaginary time direction). Thus, the relations between H, L on one side and μ, T on the other, read

$$H = \frac{e}{2\pi}\mu , \quad L = \frac{\hbar c}{k_B T} . \quad (4.1)$$

Taking the box cubic and sending $L \rightarrow \infty$, corresponds to computing the quantum partition function for the 2-dimensional SFT at zero temperature. While the relations in Eq. (4.1) have been expressed in a canonical ensemble with respect to H, μ , it should be clear that the correspondence remains true also in a microcanonical ensemble (i.e., fixed magnetic flux in SQED / fixed particle number in SFT), with a proper choice of boundary conditions.

Implications for the type I region. In the type I region of SQED, vortices attract each other. Therefore, if we are in the broken symmetry phase and force a magnetic flux through the system, the vortices form a flux tube that penetrates through the Meissner phase. What is the analogue for this in SFT? The type I region corresponds to $\tilde{\lambda} < 0$ (and the presence of further stabilising terms), and as is well known, in this case the system admits non-topological soliton solutions [50, 51], or droplets of Bose liquid, to be intuitively thought of as non-dispersive bound states of particles held together by the attractive interaction. We thus observe a perfect analogy, with the role of flux quanta in SQED played by the attractive particles in SFT. Note that even though SFT appears in a (2+1 dimensional imaginary time)

relativistic form in Eqs. (2.14), (2.15), the same solutions appear there even if we approach the non-relativistic limit [51, 52], a situation also familiar from actual experiments with soliton-like structures in superfluid Helium (see, e.g., Ref. [53]) and atomic Bose-Einstein condensates (see, e.g., Ref. [54]).

Implications for the type II region. In the type II region of SQED, on the other hand, vortices repel each other. Therefore, if we place the system in a magnetic field, they form (at least on the mean field level) an Abrikosov vortex lattice. It has been a long-standing issue to study whether, within SQED, the vortex lattice indeed exists in a strict sense for low enough magnetic fields, and then melts to a vortex liquid possibly through a first order transition, as observed experimentally [55], or always appears in a liquid state due to fluctuations, so that the transition observed in experiments would be a manifestation of some physics beyond the pure SQED (see, e.g., Ref. [56]). We now see that on the side of SFT, this corresponds to whether a 2-dimensional dilute system of atoms with repulsive interactions, forms a lattice, or melts due to quantum and thermal fluctuations. In principle, this issue could be studied with SFT, more easily than directly with SQED as attempted in Ref. [23], since the system has fewer dynamical length scales. In practice, though, the inclusion of a chemical potential in SFT makes the action complex for a generic configuration (this is just the generic “sign problem” for $\mu \neq 0$), rendering importance sampling ineffective.

5. Conclusions

In this paper, we have used numerical lattice Monte Carlo simulations to measure a number of critical exponents in three-dimensional scalar electrodynamics (SQED) in the type II region, or $\lambda/e^2 \gtrsim 1$. We have also reiterated which exponents of the dual scalar field theory (SFT) they should correspond to. Our measurements agree well with the SFT values, known to high accuracy from previous studies of the XY model. This provides strong “empirical” evidence for the existence of the conjectured duality between the two theories.

We have also elaborated on the qualitative implications of the duality for the case of macroscopic external magnetic fields, both in the type I and in the type II regions. Even though we have no new simulations to report in this regime, we find it remarkable that for all the known phenomena observed in SQED somewhat below the phase transition temperature, one indeed finds a perfect counterpart in 2-dimensional quantum SFT, but at a different temperature, as determined by the physical geometry of the SQED sample.

The duality predicts that the only important degrees of freedom near the transition point in SQED are vortex lines, and the quantities we have measured are sensitive to their properties. The agreement with the dual theory therefore also demonstrates that the methods we have used in these simulations give an accurate description of the dynamics of topological defects. Similar methods can also be used in more complicated theories, e.g., in the case of

magnetic monopoles in non-Abelian theories [57]. Therefore it should be possible to use these techniques to carry out similar studies in those systems.

In the past, the study of dualities has often been restricted to spin models, low dimensions, or supersymmetric theories. The reason for this has mostly been that only in these cases has one been able to carry out controllable analytic calculations to test and make use of the dualities. Our results show how the study of dualities can in principle be extended towards more realistic systems, by invoking numerical techniques to corroborate analytic arguments based on very general principles only, such as symmetries. The same numerical techniques could also be used to determine “experimentally” the mappings between the parameter sets. It should be mentioned that many other types of numerical avenues towards duality have, of course, been explored and extensively tested in the case of 4-dimensional Yang-Mills theory (see, e.g., Ref. [11] and references therein).

To conclude, let us finally recall that apart from the theoretical issues on which we have concentrated in this paper, the critical properties of three-dimensional SQED have also physical significance of their own, given that this theory is the effective theory of superconductivity [17] and of liquid crystals [58] in certain regimes, as well as of four-dimensional scalar electrodynamics at high temperatures [59, 45, 60]. Particularly in the first two of these cases, the substantial corrections to scaling that we have observed for the photon correlation length (also called the penetration depth), may also have phenomenological significance [61], given that it is difficult to probe very precisely the extreme vicinity of the transition point and that experimental samples are necessarily fairly restricted in size.

Acknowledgements

We acknowledge useful discussions, over the years, with P. de Forcrand, H. Kleinert, A. Kovner, I.D. Lawrie, D. Litim, F.S. Nogueira, R.D. Pisarski, A.M.J. Schakel, A. Sudbø, B. Svetitsky, and G.E. Volovik. This work was partly supported by the RTN network *Supersymmetry and the Early Universe*, EU contract no. HPRN-CT-2000-00152, by the ESF COSLAB programme, and by the Academy of Finland, contracts no. 77744 and 80170. A.R. was supported by Churchill College, Cambridge.

References

- [1] H.A. Kramers and G.H. Wannier, Phys. Rev. 60 (1941) 252.
- [2] R. Balian, J.M. Drouffe and C. Itzykson, Phys. Rev. D 11 (1975) 2098; C.P. Korthals Altes, Nucl. Phys. B 142 (1978) 315; T. Yoneya, Nucl. Phys. B 144 (1978) 195.
- [3] M.E. Peskin, Annals Phys. 113 (1978) 122.

- [4] S. Hands and J.B. Kogut, Nucl. Phys. B 462 (1996) 291 [hep-lat/9509072].
- [5] S.R. Coleman, Phys. Rev. D 11 (1975) 2088.
- [6] S. Mandelstam, Phys. Rev. D 11 (1975) 3026.
- [7] N. Seiberg and E. Witten, Nucl. Phys. B 426 (1994) 19; *ibid.* B 430 (1994) 485 (E) [hep-th/9407087]; *ibid.* B 431 (1994) 484 [hep-th/9408099].
- [8] C. Montonen and D.I. Olive, Phys. Lett. B 72 (1977) 117.
- [9] H. Osborn, Phys. Lett. B 83 (1979) 321.
- [10] J.M. Maldacena, Adv. Theor. Math. Phys. 2 (1998) 231 [hep-th/9711200].
- [11] G. Ripka, *Dual superconductor models of color confinement*, hep-ph/0310102.
- [12] T. Banks, R. Myerson and J.B. Kogut, Nucl. Phys. B 129 (1977) 493.
- [13] P.R. Thomas and M. Stone, Nucl. Phys. B 144 (1978) 513.
- [14] R. Savit, Phys. Rev. B 17 (1978) 1340.
- [15] C. Dasgupta and B.I. Halperin, Phys. Rev. Lett. 47 (1981) 1556.
- [16] H. Kleinert, Lett. Nuovo Cim. 35 (1982) 405; M. Kiometzis, H. Kleinert and A.M.J. Schakel, Fortsch. Phys. 43 (1995) 697 [cond-mat/9508142].
- [17] H. Kleinert, *Gauge Fields in Condensed Matter*, vol. 1 (World Scientific, Singapore, 1989).
- [18] A. Kovner, B. Rosenstein and D. Eliezer, Nucl. Phys. B 350 (1991) 325; A. Kovner, P. Kurzepa and B. Rosenstein, Mod. Phys. Lett. A 8 (1993) 1343; *ibid.* A 8 (1993) 2527 (E) [hep-th/9303144].
- [19] I.F. Herbut, J. Phys. A: Math. Gen. 30 (1997) 423 [cond-mat/9610052].
- [20] D.T. Son, JHEP 02 (2002) 023 [hep-ph/0201135].
- [21] R. Guida and J. Zinn-Justin, J. Phys. A: Math. Gen. 31 (1998) 8103 [cond-mat/9803240]; M. Hasenbusch and T. Török, J. Phys. A: Math. Gen. 32 (1999) 6361 [cond-mat/9904408]; M. Campostrini, M. Hasenbusch, A. Pelissetto, P. Rossi and E. Vicari, Phys. Rev. B 63 (2001) 214503 [cond-mat/0010360].
- [22] K. Kajantie, M. Laine, T. Neuhaus, J. Peisa, A. Rajantie and K. Rummukainen, Nucl. Phys. B 546 (1999) 351 [hep-ph/9809334].

- [23] K. Kajantie, M. Laine, T. Neuhaus, A. Rajantie and K. Rummukainen, Nucl. Phys. B 559 (1999) 395 [hep-lat/9906028].
- [24] P. Olsson and S. Teitel, Phys. Rev. Lett. 80 (1998) 1964 [cond-mat/9710200].
- [25] T. Neuhaus, A. Rajantie and K. Rummukainen, Phys. Rev. B 67 (2003) 014525 [cond-mat/0205523].
- [26] B.I. Halperin, T.C. Lubensky and S.-K. Ma, Phys. Rev. Lett. 32 (1974) 292.
- [27] R. Folk and Yu. Holovatch, J. Phys. A 29 (1996) 3409; cond-mat/9807421.
- [28] B. Bergerhoff, F. Freire, D.F. Litim, S. Lola and C. Wetterich, Phys. Rev. B 53 (1996) 5734 [hep-ph/9503334].
- [29] I. Herbut and Z. Tešanović, Phys. Rev. Lett. 76 (1996) 4588 [cond-mat/9605185].
- [30] H. Kleinert and F.S. Nogueira, Nucl. Phys. B 651 (2003) 361 [cond-mat/0104573].
- [31] J. Bartholomew, Phys. Rev. B 28 (1983) 5378.
- [32] Y. Munehisa, Phys. Lett. B 155 (1985) 159.
- [33] K. Kajantie, M. Karjalainen, M. Laine and J. Peisa, Phys. Rev. B 57 (1998) 3011 [cond-mat/9704056].
- [34] A.K. Nguyen and A. Sudbø, Phys. Rev. B 60 (1999) 15307 [cond-mat/9907385]; S. Mo, J. Hove and A. Sudbø, Phys. Rev. B 65 (2002) 104501 [cond-mat/0109260].
- [35] K. Kajantie, M. Laine, T. Neuhaus, A. Rajantie and K. Rummukainen, Nucl. Phys. B (Proc. Suppl.) 106 (2002) 959 [hep-lat/0110062].
- [36] J. March-Russell, Phys. Lett. B 296 (1992) 364 [hep-ph/9208215].
- [37] I.D. Lawrie, Nucl. Phys. B 200 (1982) 1; I.D. Lawrie and C. Athorne, J. Phys. A 16 (1983) L587.
- [38] S. Weinberg, Physica A 96 (1979) 327.
- [39] J. Gasser and H. Leutwyler, Annals Phys. 158 (1984) 142; Nucl. Phys. B 250 (1985) 465.
- [40] J.I. Kapusta, *Finite Temperature Field Theory* (Cambridge University Press, Cambridge, 1989).
- [41] B.D. Josephson, Phys. Lett. 21 (1966) 608; M.E. Fisher, M.N. Barber and D. Jasnow, Phys. Rev. A 8 (1973) 1111.
- [42] T. Appelquist and R.D. Pisarski, Phys. Rev. D 23 (1981) 2305.

- [43] J. Hove and A. Sudbø, Phys. Rev. Lett. 84 (2000) 3426 [cond-mat/0002197].
- [44] A.M. Polyakov, Phys. Lett. B 59 (1975) 82; Nucl. Phys. B 120 (1977) 429.
- [45] K. Kajantie, M. Karjalainen, M. Laine and J. Peisa, Nucl. Phys. B 520 (1998) 345 [hep-lat/9711048].
- [46] M. Laine and A. Rajantie, Nucl. Phys. B 513 (1998) 471 [hep-lat/9705003].
- [47] G.D. Moore, Nucl. Phys. B 523 (1998) 569 [hep-lat/9709053].
- [48] A.M. Ferrenberg and R.H. Swendsen, Phys. Rev. Lett. 63 (1989) 1195.
- [49] E. Marinari and G. Parisi, Europhys. Lett. 19 (1992) 451 [hep-lat/9205018].
- [50] G. Rosen, J. Math. Phys. 9 (1968) 996; R. Friedberg, T.D. Lee and A. Sirlin, Phys. Rev. D 13 (1976) 2739.
- [51] T.D. Lee and Y. Pang, Phys. Rept. 221 (1992) 251, and references therein.
- [52] K. Enqvist and M. Laine, JCAP 08 (2003) 003 [cond-mat/0304355].
- [53] G.E. Volovik, *The Universe in a Helium Droplet*, Chapter 3.3 (Clarendon Press, Oxford, 2003); V.V. Dmitriev, V.B. Eltsov, M. Krusius, J.J. Ruohio and G.E. Volovik, Phys. Rev. B 59 (1999) 165 [cond-mat/9805119].
- [54] L. Khaykovich *et al.*, Science 296 (2002) 1290 [cond-mat/0205378]; K.E. Strecker *et al.*, Nature 417 (2002) 150 [cond-mat/0204532].
- [55] E. Zeldov *et al.*, Nature 375 (1995) 373; A. Schilling *et al.*, Nature 382 (1996) 791.
- [56] A.K. Kienappel and M.A. Moore, Phys. Rev. B 60 (1999) 6795 [cond-mat/9809317], and references therein.
- [57] A.C. Davis, T.W.B. Kibble, A. Rajantie and H. Shanahan, JHEP 11 (2000) 010 [hep-lat/0009037]; A.C. Davis, A. Hart, T.W.B. Kibble and A. Rajantie, Phys. Rev. D 65 (2002) 125008 [hep-lat/0110154].
- [58] P.G. de Gennes, Solid State Commun. 10 (1972) 753; B.I. Halperin and T.C. Lubensky, *ibid.* 14 (1974) 997.
- [59] K. Farakos, K. Kajantie, K. Rummukainen and M. Shaposhnikov, Nucl. Phys. B 425 (1994) 67 [hep-ph/9404201].
- [60] J.O. Andersen, Phys. Rev. D 59 (1999) 065015.
- [61] S. Kamal *et al.*, Phys. Rev. Lett. 73 (1994) 1845; S. Kamal *et al.*, Phys. Rev. B 58 (1998) R8933; K.M. Paget, B.R. Boyce and T.R. Lemberger, Phys. Rev. B 59 (1999) 6545.